# A New Process Control Chart for Monitoring Short-Range Serially Correlated Data

Peihua Qiu[1], Wendong Li[2] and Jun Li[3]

[1]Department of Biostatistics, University of Florida, Gainesville, FL 32610, USA

[2]School of Statistics, East China Normal University, Shanghai, China

[3]Department of Statistics, University of California at Riverside, USA

**Abstract**

Statistical process control (SPC) charts are critically important for quality control and management in manufacturing industries, environmental monitoring, disease surveillance and many other applications. Conventional SPC charts are designed for cases when process observations are independent at different observation times. In practice, however, serial data correlation almost always exists in sequential data. It has been well demonstrated in the literature that control charts designed for independent data are unstable for monitoring serially correlated data. Thus, it is important to develop control charts specifically for monitoring serially correlated data. To this end, there is some existing discussion in the SPC literature. Most existing methods are based on parametric time series modeling and residual monitoring, where the data are often assumed to be normally distributed. In applications, however, the assumed parametric time series model with a given order and the normality assumption are often invalid, resulting in unstable process monitoring. Although there is some nice discussion on robust design of such residual monitoring control charts, the suggested designs can only handle certain special cases well. In this paper, we try to make another effort by proposing a novel control chart that makes use of the restarting mechanism of a CUSUM chart and the related spring length concept. Our proposed chart uses observations within the spring length of the current time point and ignores all history data that are beyond the spring length. It does not require any parametric time series model and/or a parametric process distribution. It only requires the assumption that process observation at a given time point is associated with nearby observations and independent of observations that are far away in observation times, which should be reasonable for many applications. Numerical studies show that it performs well in different cases.

*Key Words:* Covariance matrix decomposition; Data correlation; Decorrelation; Process monitoring; Spring length; Statistical process control.

# 1 Introduction

Statistical process control (SPC) charts have broad applications in manufacturing industries, environmental monitoring and improvement, disease surveillance, and more. Traditional SPC charts, including the Shewhart, cumulative sum (CUSUM), exponentially weighted moving averaging (EWMA), and change-point detection (CPD) charts, are designed for cases when process observations are independent at different time points (cf., Hawkins and Olwell 1998, Montgomery 2012, Qiu 2014). In practice, however, process observations at different time points are almost always correlated with each other. It has been well demonstrated in the literature that traditional SPC charts designed for independent observations are unreliable to use in cases with serially correlated data (e.g., Harris and Ross 1991, Johnson and Bagshaw 1974). Therefore, it is important to develop new control charts that are appropriate for monitoring serially correlated data, which is the focus of this paper.

In the literature, there has been some discussion on process monitoring of serially correlated data. Most existing methods on this topic are based on parametric time series modeling and sequential monitoring of the residuals. See, for instance, Apley and Shi (1999), Apley and Tsung (2002), Berthouex et al. (1978), Loredo et al. (2002), Montgomery and Mastrangelo (1991), Runger and Willemain (1995), Vander Wiel (1996), Wardell et al. (1994), and more. One common limitation of these residual-based charts is that their performance is sensitive to the assumed parametric time series models. In practice, the assumed parametric time series models could be invalid, resulting in unreliable process monitoring. Adams and Tseng (1998), Apley and Lee (2003, 2008), Apley and Tsung (2002), Lee and Apley (2011) and some other papers have discussed about the robustness of the residual-based charts, and some adjustments on the design of certain residual-based charts have been proposed. For instance, Lee and Apley (2011) suggested adjusting the control limit of the conventional EWMA chart by accommodating the uncertainty in the estimated time series models. While these adjustments represent a good research effort to overcome the major limitation of the residual-based charts, they are still based on the assumed parametric time series models with fixed orders and would not provide a reliable process monitoring in cases when the assumed models are invalid. Capizzi and Masarotto (2008) suggested a CPD chart based on a window-limited generalized likelihood ratio test for monitoring serially correlated data. The major benefits to use that CPD chart are that (i) the chart can accommodate the uncertainty about the underlying time series model by using a bootstrap resampling procedure to determine its

control limit, and (ii) the shift location and magnitude can be estimated immediately after a shift is detected. However, to specify the likelihood function, that method needs to assume a parametric time series model (i.e., ARMA) and a parametric process distribution (i.e., normal). Thus, its performance depends heavily on the validity of these model assumptions. Some researchers describe the serially correlated data by Gaussian Process (GP) models (e.g., Alshraideh and Khatatbeh 2014). These GP models assume that all process observations by the current time point during process monitoring has a joint normal distribution with a specific parameterized covariance matrix, which is difficult to justify in practice. Some other researchers suggested adjusting the control limits of conventional control charts for monitoring serially correlated data (e.g., Kim et al. 2007, Runger 2002, Schimd and Schöne 1997). However, proper adjustments of the control limits still require some prior information about the correlation structure (e.g., a parametric time series model) in the original data, which is often unavailable in practice. Another control chart suggested for monitoring stationary serially correlated data was suggested in Zhang (1998), where an EWMA chart was used and the variability of the charting statistic was estimated from an in-control (IC) dataset for determining the control limit. This chart was designed as a Shewhart chart in Zhang (1998), and the serial data correlation was considered only in determining the control limit. In practice, most processes to monitor are multivariate, and there are many control charts suggested for monitoring multivariate serially correlated data. See papers such as Bakshi (1998), Komulainen et al. 2004, Ku et al. (1995), Negiz and Cinar (1997), Rato and Reis (2013), Reis et al. (2008), Simoglou et al. (1999), Treasure et al. (2004), and more. For monitoring correlated discrete data (e.g., binary or count data), see papers such as He et al. (2016), Weiß (2015), and the references cited therein.

In this paper, we try to make another effort in tackling the important SPC problem for monitoring serially correlated data. For simplicity, our method focuses on cases when process observations are univariate and continuous numerical. In our proposed method, we suggest estimating the correlation structure nonparametrically from an IC dataset, and decorrelating the original process observations within the spring length of the current observation time before a control chart is applied, to avoid extensive computation and a large data storage requirement. The spring length is defined as the time length between the current observation time and the previous time point when a CUSUM applied to the original process observations is reset to zero (cf., Chatterjee and Qiu 2009). The concept of spring length is useful here because past observations beyond the spring length of the current observation time would not provide much useful information for process shift detection and

thus they can be ignored. After data decorrelation, we apply the conventional CUSUM chart to the decorrelated data within the spring length of the current observation time. The resulting chart is equivalent to a CUSUM on the standardized residuals of a collection of autoregressive (AR) models whose orders are $0, 1, \ldots, \widetilde{T}_{i-1}$, respectively, where $\widetilde{T}_{i-1}$ is the spring length defined in Section 2. It should be pointed out that we are not the first one to consider monitoring standardized residuals of a collection of AR models. As a matter of fact, the autoregressive $T^2$ control chart proposed in Apley and Tsung (2002) has that explanation. The differences between the two methods are that: (i) the highest order of the collection of AR models is fixed in Apley and Tsung (2002), while it is $\widetilde{T}_{i-1}$ here that may change its value over time, and (ii) the chart in Apley and Tsung (2002) is a Shewhart chart and our proposed chart is a CUSUM chart. Because the spring length $\widetilde{T}_{i-1}$ suggests that the observed data beyong the spring length can be ignored in subsequent process monitoring, it should be more reasonable to use $\widetilde{T}_{i-1}$ as the highest order of the AR models. Another benefit to decorrelate the original process observations within the spring length can be described as follows. The decorrelated observation at the current time point is usually a linear combination of the current and past observations. So, a process mean shift in the original observations would be attenuated during data decorrelation, which is a price to pay for obtaining a sequence of uncorrelated observations. The shift attenuation will negatively affect the performance of a control chart that is applied to the decorrelated data, and this negative impact is reduced by using the spring length because the spring length is usually a small integer number. The only required assumptions of the proposed method are that the IC process observations are covariance stationary and the serial autocorrelation among them is short-range in the sense that process observation at a given time point is correlated with nearby observations only and independent of observations that are quite far away in observation times, which should be reasonable for many applications.

The remainder of the article is organized as follows. Our proposed method is described in detail in Section 2. Some numerical studies for evaluating its performance are presented in Section 3. A real-data example is discussed in Section 4. Some remarks conclude the article in Section 5.

## 2 Online Monitoring of Serially Correlated Data

The basic idea of our proposed method is to decorrelate process observations before a control chart is used, without requiring a parametric time series model and a parametric process distribution. To estimate the serial data correlation structure and other IC properties (e.g., IC mean and variance) of the underlying process, it is assumed that an IC dataset $\boldsymbol{X}_{IC} = \{X_{-m+1}, ..., X_0\}$ is available. Then, the IC mean and variance can be estimated by the sample mean and variance of the IC dataset, respectively, denoted as $\widehat{\mu}_0$ and $\widehat{\sigma}^2$. Furthermore, it is assumed that the IC process observations are covariance stationary and the serial correlation exists only when two observations are within $T_{max} > 0$ in their observation indices. More specifically, it is assumed that $\gamma(q) = Cov(X_i, X_{i+q})$ only depends on $q$ when $i$ changes, and $\gamma(q) = 0$ when $q > T_{max}$, where $X_i$ and $X_{i+q}$ are two process observations obtained at times $i$ and $i + q$ when the process is IC. In practice, the autocorrelation between $X_i$ and $X_{i+q}$ usually decays when $q$ increases (e.g., stationary AR models). In such cases, $\gamma(q)$ is small when $q$ is large, and thus a proper value of $T_{max}$ can be chosen such that $\gamma(q) \approx 0$ when $q > T_{max}$. Therefore, the above assumptions should be reasonable for most manufacturing applications, as long as $T_{max}$ is not chosen too small. Then, $\gamma(q)$ can be estimated from the IC data by

$$\widehat{\gamma}_m(q) = \frac{1}{m-q} \sum_{i=-m+1}^{-q} (X_i - \widehat{\mu}_0)(X_{i+q} - \widehat{\mu}_0), \qquad \text{for } 1 \le q \le T_{max}.$$

For convenience in notation, we define $\widehat{\gamma}_m(0) = \widehat{\sigma}^2$. Obviously, the IC sample size $m$ should be larger than $T_{max}$. Note that we do not impose any parametric form on the process distribution. Thus, the above moment estimation of $\gamma(q)$ should be reasonable.

Let $X_1, X_2, \ldots$ be the Phase II observations for online monitoring. They are serially correlated as in the IC dataset. This paper focuses on detection of a mean shift as soon as possible in the Phase II observations, although detection of a variance shift can be discussed similarly after a proper variance monitoring chart (e.g., Yeh et al. 2010) substitutes the mean monitoring chart discussed in this paper. As mentioned above, Phase II observations need to be serially decorrelated before online monitoring by our proposed control chart. The computing demand in data decorrelation could be high if every new observation needs to be decorrelated with its previous $T_{max}$ observations, especially when $T_{max}$ is chosen large. To overcome this difficulty, we suggest using the concept of *spring length* that was first discussed in Chatterjee and Qiu (2009) defined below. Let $X_i$ be the observation obtained at the current time point $i$, and $C_i$ is the conventional two-sided CUSUM

charting statistic defined as

$$C_i = \max\{C_i^+, -C_i^-\}, \tag{1}$$

where

$$\begin{aligned} C_i^+ &= \max\left[0, C_{i-1}^+ + (X_i - \widehat{\mu}_0)/\widehat{\sigma} - k\right]; \\ C_i^- &= \min\left[0, C_{i-1}^- + (X_i - \widehat{\mu}_0)/\widehat{\sigma} + k\right], \text{ for } i \geq 1, \end{aligned}$$

$C_0^+ = C_0^- = 0$, and $k > 0$ is an allowance constant. One important feature of the CUSUM charting statistic $C_i$ is its re-starting mechanism. Namely, it will be reset to 0 each time when the available observations by the current time point $i$ suggest that there is little evidence of an upward or downward mean shift in the sense that $C_{i-1}^+ + (X_i - \widehat{\mu}_0)/\widehat{\sigma} \leq k$ and $C_{i-1}^- + (X_i - \widehat{\mu}_0)/\widehat{\sigma} \geq -k$ (cf., Chapter 4, Qiu 2014). Then, the spring length at time $i$ is defined as

$$T_i = \begin{cases} 0, & \text{if } C_i = 0, \\ b, & \text{if } C_i \neq 0, \ldots, C_{i-b+1} \neq 0, C_{i-b} = 0. \end{cases} \tag{2}$$

From the definition of $T_i$, it can be seen that observations that are at least $T_i$ time units before the current time point $i$ would not provide much helpful information about a future mean shift. Therefore, they can be ignored in the CUSUM chart (1), and similarly we only need to decorrelate the current observation $X_i$ with its previous $T_{i-1}$ observations. However, the above CUSUM chart (1) and the subsequent spring length $T_i$ are applied to the original observations, instead of the decorrelated ones. Also, data decorrelation depends on $T_i$. To address all these issues, the following charting procedure is suggested for online monitoring of serially correlated data.

Proposed CUSUM Chart for Monitoring Serially Correlated Data

- In the case when $i = 1$, define the standardized observation at $t_1$ to be $e_1 = (X_1 - \widehat{\mu}_0)/\sqrt{\widehat{\gamma}_m(0)}$. Then, the charting statistic at $t_1$ is defined to be

$$\widetilde{C}_1 = \max\{\widetilde{C}_1^+, -\widetilde{C}_1^-\}, \tag{3}$$

  where $\widetilde{C}_1^+ = \max\{0, e_1 - \widetilde{k}\}$, $\widetilde{C}_1^- = \min\{0, e_1 + \widetilde{k}\}$, and $\widetilde{k} > 0$ is an allowance constant. If $\widetilde{C}_1 = 0$, then define $\widetilde{T}_1 = 0$. Otherwise, define $\widetilde{T}_1 = 1$.

- In the case when $i \geq 2$, we consider the following two cases:

i) If $\widetilde{T}_{i-1} = 0$, then calculate $\widetilde{C}_i$ and $\widetilde{T}_i$ in the same way as that in the case when $i = 1$ discussed above.

ii) If $\widetilde{T}_{i-1} > 0$, define

$$\widehat{\boldsymbol{\Sigma}}_{i,i} = \begin{pmatrix} \widehat{\gamma}_m(0) & \cdots & \widehat{\gamma}_m(\widetilde{T}_{i-1}) \\ \vdots & \ddots & \vdots \\ \widehat{\gamma}_m(\widetilde{T}_{i-1}) & \cdots & \widehat{\gamma}_m(0) \end{pmatrix} = \begin{pmatrix} \widehat{\boldsymbol{\Sigma}}_{i-1,i-1} & \widehat{\boldsymbol{\sigma}}_{i-1} \\ \widehat{\boldsymbol{\sigma}}_{i-1}^T & \widehat{\gamma}_m(0) \end{pmatrix},$$

where $\widehat{\boldsymbol{\sigma}}_{i-1} = (\widehat{\gamma}_m(\widetilde{T}_{i-1}), \ldots, \widehat{\gamma}_m(1))^T$. Define

$$e_i = \frac{X_i - \widehat{\mu}_0 - \widehat{\boldsymbol{\sigma}}_{i-1}^T \widehat{\boldsymbol{\Sigma}}_{i-1,i-1}^{-1} \boldsymbol{e}_{i-1}^*}{d_i},$$

where $d_i^2 = \widehat{\gamma}_m(0) - \widehat{\boldsymbol{\sigma}}_{i-1}^T \widehat{\boldsymbol{\Sigma}}_{i-1,i-1}^{-1} \widehat{\boldsymbol{\sigma}}_{i-1}$, and $\boldsymbol{e}_{i-1}^* = (X_{i-\widetilde{T}_{i-1}} - \widehat{\mu}_0, \ldots, X_{i-1} - \widehat{\mu}_0)$. Then, according to Li and Qiu (2016), $e_i$ is asymptotically uncorrelated with $e_{i-1}, e_{i-2}, \ldots$. This result was actually derived from the Cholesky decomposition of the covariance matrix $\widehat{\boldsymbol{\Sigma}}_{i,i}$. Now, define the charting statistic to be

$$\widetilde{C}_i = \max\{\widetilde{C}_i^+, -\widetilde{C}_i^-\}, \qquad \text{for } i \geq 2, \tag{4}$$

where

$$\widetilde{C}_i^+ = \max\{0, \widetilde{C}_{i-1}^+ + e_i - \widetilde{k}\}, \qquad \widetilde{C}_i^- = \min\{0, \widetilde{C}_{i-1}^- + e_i + \widetilde{k}\}.$$

If $\widetilde{C}_i = 0$, then define $\widetilde{T}_i = 0$. Otherwise, define $\widetilde{T}_i = \min(\widetilde{T}_{i-1} + 1, T_{max})$.

- The CUSUM chart defined in (3) and (4) gives a signal of mean shift when

$$\widetilde{C}_i > \widetilde{h}, \qquad \text{for } i \geq 1, \tag{5}$$

where $\widetilde{h} > 0$ is a control limit.

In the above CUSUM chart (3)-(5), serial data decorrelation and computation of the spring length $T_i$ are implemented simultaneously, and the charting statistic $\widetilde{C}_i$ is computed from the decorrelated data. Because each decorrelated observation $e_i$ is a linear combination of the original data, its distribution would be closer to normal under some regularity conditions (cf., Wu 2011), compared to the original data. So, the CUSUM chart (3)-(5), which has some optimal properties under the normality and independent observation assumptions (cf., Chapter 4, Qiu 2014), should be more effective for monitoring the serially decorrelated data $\{e_i\}$ than for monitoring the original

data $\{X_i\}$. It should be pointed out that the quantity $e_i$ defined above can be regarded as the standardized residual of an AR time series model of order $\widetilde{T}_{i-1}$, estimated by the Yule-Walker equations (cf., Kedem and Fokianos 2002). Thus, the CUSUM chart (3)-(5) is actually a CUSUM on the standardized residuals of a collection of AR models with orders $0, 1, \ldots, \widetilde{T}_{i-1}$, respectively. As a comparison, the charting statistic of the autoregressive $T^2$ chart suggested by Apley and Tsung (2002) equals the sum of squares of the standardized residuals of a collection of AR models with orders $0, 1, \ldots, p-1$, respectively, where $p$ is a constant chosen beforehand. So, one major difference between the two methods is that the chart (3)-(5) uses $\widetilde{T}_{i-1}$ as the highest order of the collection of AR models, which may change its value over time, while the autoregressive $T^2$ chart in Apley and Tsung (2002) uses a constant $p$. Intuitively, it should be beneficial to use the spring length $\widetilde{T}_{i-1}$ here because it has been discussed above that process observations beyond the spring length can be ignored in subsequent process monitoring, which will be confirmed by some numerical examples in Section 3.

In the chart, the allowance constant $\widetilde{k}$ is usually specified in advance, and the control limit $\widetilde{h}$ can then be determined such that a pre-specified IC average run length (denoted as $ARL_0$) is reached. Because the distribution of the decorrelated data may not be exactly normal, we suggest determining $\widetilde{h}$ from the IC data. To this end, we suggest using the following bootstrap procedure that is modified from the one in Capizzi and Masarotto (2008). First, an ARMA model $X_i = \frac{\Theta(B)}{\Phi(B)} a_i$, for $i \geq 1$, is fitted from the IC data, where $B$ is a backward shift operator, $\Phi(B) = 1 - \phi_1 B - \phi_2 B^2 - \cdots - \phi_p B^{r_1}$ is an autoregressive polynomial of order $r_1$, $\Theta(B) = 1 - \theta_1 B - \theta_2 B^2 - \cdots - \theta_q B^{r_2}$ is the moving averaging polynomial of order $r_2$, and the orders $r_1$ and $r_2$ are determined by BIC. Define $\widehat{a}_i = \widehat{\Theta}^{-1}(B)\widehat{\Phi}(B)X_i$, for $i \geq 1$, as the residuals of the estimated ARMA model. Then, we draw with replacement a sample of size $M$ from the set of residuals $\{\widehat{a}_i, i = 1, 2, \ldots, m\}$, where $M > 0$ is a large enough number (e.g., $M = 10,000$ in the examples of Section 3). The drawn sample is denoted as $\{\widehat{a}_i^*, i = 1, 2, \ldots, M\}$. Then, the bootstrap sample of process observations is defined as $\{X_i^* = \frac{\widehat{\Theta}(B)}{\widehat{\Phi}(B)} \widehat{a}_i^*, i = 1, 2, \ldots, M\}$. The CUSUM chart (3)-(5) with the control limit $\widetilde{h}$ is then applied to the bootstrap sample to obtain a run length (RL) value. This bootstrap resampling procedure is repeated for $B$ times and the $B$ resulting RL values are averaged to obtain the $ARL_0$ value at the given $\widetilde{h}$ value. Then, the $\widetilde{h}$ value can be searched by a bisection algorithm or its modified versions (Capizzi and Masarotto 2016) so that the assumed $ARL_0$ value is reached. Note that this bootstrap procedure is used for determining the control limit of the proposed chart before online process monitoring; it will not add much computing burden to the proposed method. Also, note that

an ARMA model is used in the above bootstrap procedure, which is reasonable because the IC data are assumed to be a short-range covariance stationary time series and thus can be approximately described by an ARMA model according to the Wold Representation Theorem (cf., Bierens 2004). Unlike online process monitoring in which large-sample approximation results usually do not apply, determination of the control limit $\widetilde{h}$ is finished before online process monitoring and $\widetilde{h}$ is searched from a given IC dataset. As long as the size of the IC dataset is reasonably large, the ARMA model approximation should work reasonably well, which has been confirmed in our simulation (cf., Table 1 in Section 3). The above bootstrap procedure is different from the one in Capizzi and Masarotto (2008) in that it does not require the IC data to follow a normal distribution while the bootstrap samples in Capizzi and Masarotto (2008) were generated from normal distributions.

In the simulation study in Section 3, the impact of the IC data size $m$ and the maximum time range of serial autocorrelation $T_{max}$ on the performance of the control chart (3)-(5) will be discussed in different scenarios. Based on the related results, we can see that the performance of the chart is stable when $m \geq 2,000$ and $T_{max} \geq 5$.

## 3 Simulation Study

In this section, we present some simulation results regarding the performance of the proposed CUSUM chart (3)-(5) for monitoring serially correlated data. Besides the proposed CUSUM chart, denoted as NEW, we also consider the following five charts for comparison purpose.

(i) The conventional CUSUM chart, denoted as CCUSUM, has the charting statistic defined in (1). The chart gives a signal when $C_i > h$, where $h > 0$ is a control limit that is determined by the conventional bootstrap procedure (cf., Efron and Tibshirani 1993) from the IC data.

(ii) The modified EWMA chart suggested by Zhang (1998), denoted as EWMA-Z, has the charting statistic

$$E_i = (1-\lambda)E_{i-1} + \lambda X_i, \qquad \text{for } i \geq 1, \tag{6}$$

where $E_0 = \widehat{\mu}_0$, and $\lambda \in (0, 1]$ is a weighting parameter. The chart gives a signal when $E_i > \widehat{\mu}_0 + L\widehat{\sigma}_E$ or $E_i < \widehat{\mu}_0 - L\widehat{\sigma}_E$, where

$$\widehat{\sigma}_E^2 = \frac{\lambda}{2-\lambda}\widehat{\gamma}_m(0) \times \left\{1 + 2\sum_{k=1}^{M} \frac{\widehat{\gamma}_m(j)}{\widehat{\gamma}_m(0)}(1-\lambda)^j \left[1 - (1-\lambda)^{2(M-j)}\right]\right\},$$

$\{\widehat{\gamma}_m(j), 1 \le j \le M\}$ are defined in Section 2, $M > 0$ is a pre-specified integer and chosen to be 25, as recommended by the author.

(iii) The residual-based chart suggested by Lee and Apley (2011), denoted as EWMA-LA, assumes that the IC process observations follow an ARMA model $X_i = \frac{\Theta(B)}{\Phi(B)} a_i$, for $i \ge 1$, where $B$ and other notations are defined in the second last paragraph in Section 2. Define $\widehat{e}_i = \widehat{\Theta}^{-1}(B)\widehat{\Phi}(B)X_i$, for $i \ge 1$, as the residuals of the estimated ARMA model. Then, the charting statistic of EWMA-LA is defined by (6), after $X_i$ is replaced by $\widehat{e}_i$. The control limits of the chart are chosen to be $\widehat{\mu}_0 \pm L\sqrt{E[\sigma_E^2|\widehat{\gamma}]}$, where the estimated parameters $\widehat{\gamma} = [\widehat{\phi}_1, \widehat{\phi}_2, \cdots, \widehat{\phi}_{r_1}, \widehat{\theta}_1, \widehat{\theta}_2, \cdots, \widehat{\theta}_{r_2}]^T$ are obtained from the IC dataset, and the parameter $L$ is chosen such that the pre-specified $ARL_0$ is reached when $\sqrt{E[\sigma_E^2|\widehat{\gamma}]}$ is replaced by $\widehat{\sigma}_E = \widehat{\sigma}\sqrt{\lambda/(2-\lambda)}$ in its control limits and $\widehat{\sigma}$ is obtained from the IC data as discussed at the beginning of Section 2.

(iv) The CPD chart based on a window-limited generalized likelihood ratio test by Capizzi and Masarotto (2008), denoted as GLRW, is constructed based on an ARMA model with the normal distribution assumption. Its control limit is determine by a bootstrap procedure, similar to the one described in Section 2, with the bootstrap sample size being 10,000, except that the residuals $\{\widehat{a}_i^*\}$ used for generating the bootstrap samples are generated from a zero-mean normal distribution in Capizzi and Masarotto (2008).

(v) The autoregressive $T^2$ chart suggested by Apley and Tsung (2002), denoted as T2, considers the sequence of $p$-dimensional vectors $\mathbf{X}_i = (X_{i-p+1}, X_{i-p+2}, \ldots, X_i)'$, for $i \ge p$. Its Shewhart charting statistic is $T_i^2 = (\mathbf{X}_i - \boldsymbol{\mu}_0)'\Sigma_{\mathbf{X}}^{-1}(\mathbf{X}_i - \boldsymbol{\mu}_0)$, where $\boldsymbol{\mu}_0 = (\mu_0, \mu_0, \ldots, \mu_0)'$ and $\Sigma_{\mathbf{X}}$ are the IC mean and covariance matrix of $\mathbf{X}_i$ that can be estimated from the IC data. It was shown in Apley and Tsung (2002) that $T_i^2$ was the sum of the squared standardized residuals of a collection of AR models of orders $0, 1, \ldots, p-1$, respectively. The control limit of the chart is chosen to be the $1-\alpha$ percentile of the chi-square distribution with $p$ degrees of freedom, where $\alpha$ is a false alarm probability.

In all six control charts discussed above, we assume that $ARL_0 = 200$. Their IC parameters are estimated from an IC data of size $m = 2000$. For each chart, its actual $ARL_0$ value is computed as follows. First, an IC dataset is generated, and the IC parameters (e.g., $\mu_0, \gamma(q)$) are calculated from the IC data. Second, with the estimated IC parameters obtained in step 1, the average run length

(ARL) is calculated from 10,000 replicated simulations of Phase II process monitoring. Third, the previous two steps are repeated for 100 times, and the average of the 100 ARL values is used as the calculated actual $ARL_0$ value. The standard error of the calculated actual $ARL_0$ value can also be computed. In the chart NEW, we fix $T_{max}$ to be 20. In EWMA-Z and EWMA-LA, the constant $L$ can be obtained from Table 5.1 in Qiu (2014) or the R package *spc* so that the related EWMA charts have the nominal $ARL_0$ value of 200. In GLRW, the window size is set to be 20, as in the simulation in Capizzi and Masarotto (2008). For both NEW and GLRW, the bootstrap sample size is chosen to be 10,000 when determining their control limits. For T2, the parameter $p$ is chosen to be 20, and $\alpha$ is determined by the equation $\log(ARL_0) = 2.364 - 0.871\log(\alpha)$, as suggested in Apley and Tsung (2002). The following six cases of data correlation are considered:

**Case I** Observations $X_1, X_2, \ldots$ are i.i.d. when the process is IC, and the IC process distribution is $N(0,1)$;

**Case II** Process observations follow the AR(1) model $X_i = 0.5X_{i-1} + \varepsilon_i$, for $i \geq 1$, where $X_0 = 0$ and $\{\varepsilon_i, i \geq 1\}$ are i.i.d. with the distribution $N(0,1)$;

**Case III** Process observations follow the AR(2) model $X_i = 0.4X_{i-1} + 0.2X_{i-2} + \varepsilon_i$, for $i \geq 2$, where $X_0 = X_1 = 0$ and $\{\varepsilon_i, i \geq 1\}$ are i.i.d. with the distribution $t(5)$;

**Case IV** Process observations follow the model $X_i = 1.5\xi_i + \varepsilon_i$, for $i \geq 1$, where $\{\varepsilon_i, i \geq 1\}$ are i.i.d. with the distribution $N(0,1)$, and $\{\xi_i, i \geq 1\}$ is a two-state Markov point process with the initial state being 0 and the transition matrix between the two states of $\{0,1\}$ being $\begin{pmatrix} 0.8, & 0.2 \\ 0.2, & 0.8 \end{pmatrix}$;

**Case V** Process observations follow the MA(2) model $X_i = \varepsilon_i + 0.85\varepsilon_{i-1} + 0.7\varepsilon_{i-2}$, for $i \geq 2$, where $X_1 = X_2 = 0$ and $\{\varepsilon_i, i \geq 1\}$ are i.i.d. with the distribution $N(0,1)$;

**Case VI** Process observations follow the ARMA(3,1) model $X_i = 0.83X_{i-1} - 0.57X_{i-2} + 0.4X_{i-3} + \varepsilon_i - 0.5\varepsilon_{i-1}$, for $i \geq 4$, where $X_1 = X_2 = X_3 = 0$, $\{\varepsilon_i, i \geq 1\}$ are i.i.d. with the distribution $\chi^2_3$.

For each of the above six cases, the process distribution is centralized and re-scaled properly so that the IC process mean is 0 and the IC process standard deviation is 1. So, the conventional assumptions that the IC process observations are i.i.d. and normally distributed are valid in Case I.

In Case II, process observations follow the AR(1) model. So, the model assumptions in EWMA-LA and GLRW are satisfied. But, the assumptions in CCUSUM are violated. In Case III, it is assumed that the specified model in EWMA-LA is AR(1), which is violated, although the true autoregressive model is still an ARMA. This case is considered here to study the performance of EWMA-LA when its autoregressive model is mis-specified. In this case, the ARMA model assumption in GLRW is valid. However, the normal distribution assumption in CCUSUM, EWMA-LA, GLRW, and T2 is violated. The true data correlation model in Case IV is not an ARMA model. So, the model assumptions in CCUSUM, EWMA-LA and GLRW are violated. In Case V, the model assumptions in EWMA-LA and GLRW are valid, but the model assumptions in CCUSUM are violated. In Case VI, although the time series model is an ARMA, but the error distribution is $\chi^2_3$, which is skewed. So, the normal distribution assumption in EWMA-LA, GLRW and T2 are violated. In all six cases, the stationary autocorrelation assumption in EWMA-Z, NEW, and T2 are satisfied. The short-range correlation assumption is also valid or approximately valid.

**IC performance.** We first study the IC performance of the related charts in the six cases described above when no mean shifts are present and the nominal $ARL_0$ value of each chart is 200. In the two CUSUM charts CCUSUM and NEW, the allowance constants $k$ and $\widetilde{k}$ are chosen to be 0.1, 0.25 or 0.5. The weighting parameter $\lambda$ in the two EWMA charts EWMA-Z and EWMA-LA is chosen to be 0.05, 0.1 or 0.2. The orders of the ARMA model assumed in EWMA-LA and GLRW are determined by BIC, except that it is assumed to be AR(1) in case III for EWMA-LA. The control limit of each chart is chosen under its assumed model assumptions such that the nominal $ARL_0$ value of 200 is reached. The actual $ARL_0$ value of a chart is calculated by applying the chart to the IC process observations generated in each of the six cases considered, as described earlier. The calculated actual $ARL_0$ values and their standard errors of the six charts are presented in Table 1. From the table, we can make the following conclusions. (i) The conventional CUSUM chart CCUSUM has a reliable IC performance in Case I, but its IC performance is not reliable in Cases II-VI, which is intuitively reasonable, because its model assumptions are satisfied in Case I only and violated in all Cases II-VI. (ii) The chart EWMA-Z has a good performance in Case I, is conservative in cases II-V, and unreliable in Case VI. (iii) The IC performance of EWMA-LA is good in Cases II and V when its assumptions are valid, reasonably good in Case I when its assumptions are valid but the true data are independent, and unreliable in Cases III, IV and VI when its model assumptions are invalid. (iv) The chart GLRW is good in Cases I, II and V when its model assumptions are valid, and not that good in cases III, IV and VI when its time series

model and/or the normal distribution assumption are violated. (v) The overall IC performance of T2 is similar to that of GLRW, while it performs better than GLRW in Case IV when the true data correlation does not follow an ARMA model. As a comparison, the proposed chart NEW has a reliable IC performance in all cases considered.

Table 1: Calculated actual $ARL_0$ values and their standard errors (in parentheses) of six control charts in Cases I-VI.

| | CCUSUM | | EWMA-Z | | EWMA-LA | | NEW | | GLRW | T2 |
|---|---|---|---|---|---|---|---|---|---|---|
| Cases | $k$ | $ARL_0$ | $\lambda$ | $ARL_0$ | $\lambda$ | $ARL_0$ | $\widetilde{k}$ | $ARL_0$ | $ARL_0$ | $ARL_0$ |
| I | 0.1 | 202(1.73) | 0.05 | 194(3.42) | 0.05 | 185(2.63) | 0.1 | 180(2.32) | | |
| | 0.25 | 198(2.26) | 0.1 | 192(4.32) | 0.1 | 186(2.89) | 0.25 | 184(2.45) | 188(2.48) | 191(3.14) |
| | 0.5 | 203(2.41) | 0.2 | 203(4.45) | 0.2 | 184(2.75) | 0.5 | 182(2.27) | | |
| II | 0.1 | 51(0.25) | 0.05 | 240(5.64) | 0.05 | 195(3.87) | 0.1 | 196(2.29) | | |
| | 0.25 | 44(0.20) | 0.1 | 281(7.58) | 0.1 | 196(3.71) | 0.25 | 198(2.23) | 204(2.75) | 205(3.11) |
| | 0.5 | 49(0.29) | 0.2 | 319(8.02) | 0.2 | 204(3.90) | 0.5 | 199(2.35) | | |
| III | 0.1 | 44(0.24) | 0.05 | 252(5.08) | 0.05 | 129(2.15) | 0.1 | 207(2.36) | | |
| | 0.25 | 35(0.26) | 0.1 | 296(6.34) | 0.1 | 122(2.39) | 0.25 | 210(2.30) | 164(2.33) | 147(2.36) |
| | 0.5 | 37(0.35) | 0.2 | 312(6.29) | 0.2 | 119(2.10) | 0.5 | 196(2.28) | | |
| IV | 0.1 | 65(0.30) | 0.05 | 259(5.17) | 0.05 | 258(4.32) | 0.1 | 194(2.26) | | |
| | 0.25 | 60(0.31) | 0.1 | 364(8.83) | 0.1 | 277(4.88) | 0.25 | 197(2.31) | 328(5.80) | 221(3.61) |
| | 0.5 | 62(0.43) | 0.2 | 470(11.98) | 0.2 | 357(6.11) | 0.5 | 196(2.40) | | |
| V | 0.1 | 51(0.36) | 0.05 | 235(5.89) | 0.05 | 197(3.47) | 0.1 | 193(2.34) | | |
| | 0.25 | 47(0.33) | 0.1 | 287(8.04) | 0.1 | 204(3.59) | 0.25 | 192(2.39) | 193(2.61) | 208(3.49) |
| | 0.5 | 45(0.30) | 0.2 | 308(7.98) | 0.2 | 198(3.33) | 0.5 | 195(2.42) | | |
| VI | 0.1 | 484(21.88) | 0.05 | 160(3.04) | 0.05 | 151(2.11) | 0.1 | 197(2.53) | | |
| | 0.25 | 290(8.40) | 0.1 | 136(2.41) | 0.1 | 132(1.88) | 0.25 | 201(2.58) | 133(1.60) | 124(2.25) |
| | 0.5 | 128(3.65) | 0.2 | 112(1.64) | 0.2 | 114(1.52) | 0.5 | 196(2.49) | | |

**OC performance.** Next, we study the OC performance of the related charts in the six different cases discussed above. In each case, a shift is assumed to occur at the beginning of Phase II process monitoring, with the shift size being $\delta\sigma_X$ and $\delta$ changing among 0, 0.25, 0.5, 0.75 and 1.0 (the process is actually IC when the shift size is 0). To make the comparison among different charts fair, we have adjusted the control limits of all charts so that their actual $ARL_0$ values are 200 when $\delta = 0$. First, we compute the *optimal* $ARL_1$ values of the four charts CCUSUM,

EWMA-Z, EWMA-LA and NEW for detecting each shift, where the optimal $ARL_1$ value of a chart is obtained by changing the allowance constant $k$ or $\widetilde{k}$ in the two CUSUM charts CCUSUM and NEW or the weighting parameter $\lambda$ in the two EWMA charts EWMA-Z and EWMA-LA, such that the $ARL_1$ value is minimized for detecting each shift while the actual $ARL_0$ value is maintained at 200. Because the charts GLRW and T2 do not have such a smoothing parameter to choose, they are not included in this comparison. Otherwise, the comparison would be unfair to GLRW and T2. The optimal $ARL_1$ values are considered here to make the comparison among the four charts as fair as possible. Otherwise, the OC performance of CCUSUM with $k = 0.1$ may not be comparable to the OC performance of EWMA-LA when $\lambda = 0.1$, and so forth. The calculated optimal $ARL_1$ values of the four charts are presented in Table 2. From the table, it can be seen that (i) the four charts perform similarly in Case I, (ii) EWMA-LA is slight better than the other three charts in Cases II and V, and (iii) the proposed chart NEW is uniformly better than the other three charts in Cases III, IV and VI, except that it performs slightly worse than EWMA-Z in Case IV when $\delta = 0.75$. The conclusion (ii) is reasonable because the assumed parametric time series model and the normality assumption in EWMA-LA are valid in Cases II and V. So, EWMA-LA would be more efficient than the other three charts in such cases. In cases III, IV and VI, the performance of EWMA-LA is unsatisfactory because its parametric time series model is mis-specified in Case III, invalid in Case IV, and its normality assumption is invalid in Cases III and VI. The values of the smoothing parameters $k$, $\widetilde{k}$ and $\lambda$ at which the optimal $ARL_1$ values in Table 2 are reached are presented in Table 3. It can be seen that indeed different charts should choose different values of their smoothing parameters.

Next, we compare the OC performance of all six control charts by specifying the smoothing parameters $k$, $\widetilde{k}$ and $\lambda$ in the four charts CCUSUM, EWMA-Z, EWMA-LA and NEW to be 0.1, 0.25 and 0.5, the window parameter in GLRW to be 20 (as in the simulation examples in Capizzi and Masarotto (2008)), $p = 20$ in T2, and other setups are kept the same as those in the example of Table 2. The results are presented in Table 4. From the table, it seems that (i) T2 performs relatively poor in all cases considered because it is a Shewhart chart and other charts are either CUSUM or EWMA charts, (ii) all charts, except T2, perform reasonably well in Case I, (iii) the chart EWMA-LA has an overall better performance in Cases II and V when its model assumptions are satisfied, and (iv) the chart NEW has an overall better performance in the remaining three cases III, IV and VI. These conclusions are consistent with those in Table 2.

Table 2: Calculated optimal $ARL_1$ values and their standard errors of the four charts when $ARL_0 = 200$ and the shift size $\delta$ changes among 0.25, 0.5, 0.75 and 1.0. The optimal $ARL_1$ value of a chart is obtained by changing the allowance constant $k$ or $\widetilde{k}$ in the two CUSUM charts CCUSUM and NEW or the weighting parameter $\lambda$ in the two EWMA charts EWMA-Z and EWMA-LA, such that the $ARL_1$ value is minimized for detecting each shift while the actual $ARL_0$ value is maintained at 200. Numbers in bold are the smallest ones in individual rows.

| Cases | $\delta$ | CCUSUM | EWMA-Z | EWMA-LA | NEW |
|---|---|---|---|---|---|
| I | 0.25 | **58.63**(0.40) | 59.13(0.38) | 60.17(0.40) | 58.81(0.39) |
| | 0.50 | **23.90**(0.14) | 24.58(0.14) | 24.83(0.13) | 24.33(0.14) |
| | 0.75 | **13.36**(0.07) | 13.48(0.07) | 13.97(0.08) | 13.48(0.07) |
| | 1.00 | 8.62(0.04) | 9.02(0.04) | 9.44(0.04) | **8.58**(0.04) |
| II | 0.25 | 106.95(0.73) | 103.63(0.81) | **92.66**(0.65) | 99.24(0.76) |
| | 0.50 | 50.58(0.33) | 49.58(0.32) | **44.77**(0.26) | 47.34(0.28) |
| | 0.75 | 29.19(0.20) | 29.62(0.16) | **26.31**(0.14) | 28.66(0.18) |
| | 1.00 | 18.82(0.11) | 18.62(0.11) | 18.43(0.09) | **18.36**(0.10) |
| III | 0.25 | 110.63(0.81) | 114.96(0.90) | 160.06(1.39) | **98.25**(0.63) |
| | 0.50 | 57.31(0.38) | 59.26(0.43) | 81.08(0.58) | **53.29**(0.35) |
| | 0.75 | 34.56(0.24) | 35.78(0.25) | 45.80(0.31) | **32.30**(0.22) |
| | 1.00 | 23.36(0.14) | 24.16(0.12) | 31.55(0.15) | **23.12**(0.14) |
| IV | 0.25 | 101.58(0.84) | 96.16(0.81) | 90.87(0.64) | **82.19**(0.57) |
| | 0.50 | 40.59(0.33) | 38.27(0.30) | 40.14(0.27) | **35.54**(0.30) |
| | 0.75 | 20.79(0.18) | **20.14**(0.16) | 21.56(0.13) | 20.26(0.16) |
| | 1.00 | 12.88(0.10) | 12.75(0.09) | 14.39(0.09) | **12.30**(0.10) |
| V | 0.25 | 116.54(0.88) | 113.41(0.86) | **92.10**(0.68) | 95.18(0.66) |
| | 0.50 | 52.81(0.38) | 50.05(0.36) | **44.29**(0.28) | 47.20(0.29) |
| | 0.75 | 30.22(0.19) | 27.93(0.18) | **26.37**(0.17) | 27.05(0.18) |
| | 1.00 | 19.51(0.12) | 18.69(0.12) | **17.89**(0.11) | 18.28(0.13) |
| VI | 0.25 | 41.24(0.19) | 38.43(0.20) | 37.92(0.18) | **33.53**(0.16) |
| | 0.50 | 18.78(0.08) | 16.35(0.07) | 16.85(0.06) | **14.58**(0.07) |
| | 0.75 | 11.91(0.04) | 10.88(0.04) | 11.05(0.04) | **9.10**(0.03) |
| | 1.00 | 8.49(0.03) | 7.62(0.03) | 8.12(0.03) | **6.49**(0.03) |

Table 3: Values of the smoothing parameters $k$, $\widetilde{k}$ and $\lambda$ at which the optimal $ARL_1$ values in Table 2 are reached.

| | | CCUSUM | EWMA-Z | EWMA-LA | NEW |
|---|---|---|---|---|---|
| Cases | $\delta$ | $k$ | $\lambda$ | $\lambda$ | $\tilde{k}$ |
| I | 0.25 | 0.125 | 0.02 | 0.01 | 0.15 |
| | 0.50 | 0.25 | 0.05 | 0.05 | 0.25 |
| | 0.75 | 0.375 | 0.1 | 0.1 | 0.35 |
| | 1.00 | 0.5 | 0.2 | 0.2 | 0.5 |
| II | 0.25 | 0.1 | 0.02 | 0.01 | 0.1 |
| | 0.50 | 0.25 | 0.03 | 0.02 | 0.15 |
| | 0.75 | 0.4 | 0.05 | 0.035 | 0.25 |
| | 1.00 | 0.5 | 0.1 | 0.05 | 0.35 |
| III | 0.25 | 0.15 | 0.01 | 0.02 | 0.05 |
| | 0.50 | 0.25 | 0.025 | 0.03 | 0.1 |
| | 0.75 | 0.4 | 0.04 | 0.05 | 0.15 |
| | 1.00 | 0.5 | 0.06 | 0.08 | 0.2 |
| IV | 0.25 | 0.25 | 0.05 | 0.025 | 0.1 |
| | 0.50 | 0.5 | 0.1 | 0.05 | 0.3 |
| | 0.75 | 0.75 | 0.2 | 0.1 | 0.5 |
| | 1.00 | 1.0 | 0.25 | 0.2 | 0.75 |
| V | 0.25 | 0.2 | 0.02 | 0.01 | 0.1 |
| | 0.50 | 0.3 | 0.04 | 0.03 | 0.2 |
| | 0.75 | 0.4 | 0.07 | 0.06 | 0.3 |
| | 1.00 | 0.5 | 0.1 | 0.1 | 0.4 |
| VI | 0.25 | 0.1 | 0.025 | 0.025 | 0.05 |
| | 0.50 | 0.2 | 0.05 | 0.05 | 0.2 |
| | 0.75 | 0.3 | 0.075 | 0.1 | 0.4 |
| | 1.00 | 0.4 | 0.1 | 0.2 | 0.6 |

Table 4: Calculated $ARL_1$ values and their standard errors (in parentheses) of the six charts when $ARL_0 = 200$ and the shift size $\delta$ changes among 0.25, 0.5, 0.75 and 1.0. Numbers in bold are the smallest ones in individual rows.

| | | CCUSUM | | | EWMA-Z | | | EWMA-LA | | | NEW | | | GLRW | T2 |
|---|---|---|---|---|---|---|---|---|---|---|---|---|---|---|---|
| | | $k$ | | | $\lambda$ | | | $\lambda$ | | | $\tilde{k}$ | | | | |
| Cases | $\delta$ | 0.1 | 0.25 | 0.5 | 0.05 | 0.1 | 0.2 | 0.05 | 0.1 | 0.2 | 0.1 | 0.25 | 0.5 | | |
| I | 0.25 | 60.24(0.41) | 68.91(0.55) | 84.12(0.75) | 62.57(0.46) | 68.49(0.58) | 83.44(0.78) | 63.11(0.48) | 68.90(0.59) | 83.52(0.77) | **59.94**(0.42) | 69.12(0.57) | 84.81(0.77) | 73.65(0.62) | 155.95(1.42) |
| | 0.50 | 27.30(0.14) | **23.98**(0.14) | 27.89(0.22) | 24.58(0.13) | 26.01(0.16) | 28.89(0.23) | 24.88(0.13) | 26.59(0.16) | 29.39(0.24) | 27.56(0.15) | 24.33(0.14) | 28.30(0.23) | 28.35(0.23) | 84.08(0.71) |
| | 0.75 | 17.52(0.10) | 14.45(0.06) | 14.08(0.08) | 14.13(0.07) | **13.58**(0.06) | 14.88(0.08) | 14.71(0.08) | 14.05(0.07) | 15.43(0.08) | 17.83(0.10) | 14.59(0.06) | 14.37(0.08) | 15.50(0.10) | 42.85(0.30) |
| | 1.00 | 13.11(0.05) | 10.27(0.04) | 8.62(0.03) | 10.07(0.04) | 9.55(0.03) | 8.97(0.03) | 10.64(0.05) | 10.03(0.04) | 9.48(0.04) | 13.54(0.05) | 10.79(0.04) | **8.58**(0.04) | 10.25(0.05) | 26.11(0.11) |
| II | 0.25 | 106.95(0.73) | 108.89(0.88) | 123.18(1.11) | 107.01(0.93) | 119.41(1.09) | 134.66(1.27) | **96.71**(0.82) | 109.11(0.98) | 129.42(1.24) | 99.24(0.76) | 122.39(1.01) | 136.23(1.10) | 121.48(1.10) | 165.96(1.52) |
| | 0.50 | 54.37(0.28) | 50.58(0.33) | 54.68(0.44) | 50.65(0.36) | 52.34(0.43) | 63.11(0.57) | **47.03**(0.32) | 51.80(0.41) | 63.51(0.57) | 48.90(0.27) | 53.29(0.40) | 68.67(0.55) | 58.82(0.43) | 110.10(0.98) |
| | 0.75 | 35.40(0.14) | 29.45(0.16) | 31.05(0.21) | 29.62(0.16) | 30.82(0.20) | 32.36(0.27) | **27.35**(0.15) | 28.96(0.20) | 35.41(0.29) | 30.24(0.15) | 28.66(0.18) | 35.32(0.26) | 35.27(0.25) | 65.57(0.54) |
| | 1.00 | 25.27(0.09) | 21.57(0.09) | 18.82(0.11) | 19.08(0.09) | 18.62(0.11) | 20.45(0.15) | **18.43**(0.09) | 19.11(0.11) | 22.00(0.16) | 23.18(0.08) | 19.52(0.11) | 21.23(0.15) | 20.88(0.10) | 41.22(0.29) |
| III | 0.25 | 112.58(0.77) | 115.03(0.92) | 126.24(1.17) | 126.53(1.12) | 134.96(1.24) | 153.62(1.48) | 180.79(1.60) | 184.58(1.75) | 188.30(1.80) | **101.48**(0.77) | 130.23(1.19) | 154.77(1.39) | 179.21(1.74) | 182.79(1.72) |
| | 0.50 | 61.29(0.33) | 57.31(0.38) | 62.74(0.51) | 61.52(0.50) | 71.55(0.63) | 94.03(0.78) | 84.30(0.68) | 96.59(0.85) | 120.76(1.09) | **53.29**(0.35) | 68.24(0.58) | 101.82(0.90) | 146.84(1.40) | 154.57(1.40) |
| | 0.75 | 40.59(0.18) | 35.77(0.20) | 35.49(0.26) | 36.77(0.24) | 39.60(0.31) | 50.00(0.43) | 45.80(0.31) | 50.51(0.41) | 71.93(0.58) | **34.39**(0.19) | 38.56(0.29) | 60.46(0.54) | 100.37(0.92) | 117.28(1.00) |
| | 1.00 | 29.30(0.11) | 25.08(0.12) | **23.36**(0.14) | 24.57(0.12) | 25.85(0.15) | 29.90(0.24) | 32.03(0.15) | 34.56(0.22) | 42.17(0.32) | 24.26(0.12) | 25.50(0.17) | 38.49(0.31) | 52.12(0.42) | 88.10(0.69) |
| IV | 0.25 | 102.25(0.69) | 101.58(0.84) | 103.55(0.93) | 96.16(0.81) | 98.95(0.90) | 104.74(0.99) | 91.90(0.73) | 94.00(0.82) | 99.31(0.90) | **82.19**(0.57) | 84.06(0.71) | 90.00(0.83) | 104.28(0.96) | 164.07(1.52) |
| | 0.50 | 46.77(0.24) | 42.15(0.29) | 40.59(0.33) | 38.99(0.27) | 38.27(0.30) | 39.32(0.34) | 40.14(0.27) | 41.47(0.30) | 43.82(0.34) | 39.89(0.22) | **36.68**(0.28) | 37.32(0.32) | 43.24(0.36) | 98.78(0.86) |
| | 0.75 | 28.33(0.12) | 24.36(0.13) | 21.87(0.16) | 22.28(0.13) | 20.76(0.14) | **20.14**(0.16) | 22.69(0.11) | 21.56(0.13) | 21.94(0.15) | 25.40(0.11) | 21.71(0.14) | 20.26(0.16) | 23.96(0.18) | 54.18(0.42) |
| | 1.00 | 21.22(0.07) | 16.66(0.08) | 14.26(0.09) | 15.27(0.07) | 13.67(0.08) | 12.98(0.09) | 16.10(0.07) | 14.94(0.08) | 14.39(0.09) | 18.31(0.07) | 14.55(0.08) | **12.89**(0.10) | 15.93(0.10) | 33.25(0.20) |
| V | 0.25 | 117.78(0.84) | 120.19(1.00) | 132.50(1.19) | 116.74(1.04) | 129.00(1.20) | 143.10(1.39) | 101.91(0.90) | 112.64(1.06) | 132.61(1.36) | **95.18**(0.66) | 104.57(0.91) | 124.23(1.19) | 139.11(1.43) | 167.60(1.56) |
| | 0.50 | 56.55(0.31) | 53.24(0.37) | 59.33(0.50) | 50.41(0.38) | 55.79(0.48) | 66.44(0.61) | **45.22**(0.33) | 49.28(0.42) | 61.80(0.61) | 47.82(0.26) | 47.95(0.35) | 60.47(0.55) | 67.42(0.68) | 115.02(1.02) |
| | 0.75 | 35.64(0.15) | 30.74(0.17) | 31.44(0.23) | 28.15(0.17) | 29.24(0.22) | 34.37(0.29) | **26.57**(0.16) | 27.07(0.20) | 31.84(0.29) | 30.74(0.14) | 27.39(0.17) | 31.82(0.26) | 34.07(0.32) | 72.10(0.60) |
| | 1.00 | 25.90(0.09) | 21.12(0.10) | 19.51(0.12) | 19.04(0.10) | 18.69(0.12) | 20.54(0.16) | 18.48(0.09) | **17.89**(0.11) | 19.33(0.15) | 22.48(0.09) | 18.60(0.10) | 19.20(0.14) | 19.88(0.17) | 45.78(0.33) |
| VI | 0.25 | 41.24(0.19) | 52.18(0.37) | 260.18(2.55) | 40.34(0.25) | 70.42(0.59) | 599.10(6.07) | 38.48(0.21) | 44.07(0.32) | 210.54(2.01) | **35.18**(0.19) | 39.21(0.27) | 89.38(0.80) | 282.99(2.77) | 145.43(1.35) |
| | 0.50 | 20.61(0.06) | 19.53(0.09) | 34.51(0.24) | 16.35(0.07) | 18.89(0.10) | 57.68(0.48) | 16.85(0.06) | 17.45(0.07) | 24.19(0.15) | 19.01(0.06) | **15.33**(0.07) | 19.70(0.11) | 53.51(0.41) | 97.14(0.89) |
| | 0.75 | 13.59(0.04) | 12.20(0.04) | 14.92(0.07) | 11.15(0.04) | 11.33(0.04) | 14.35(0.08) | 11.48(0.04) | 11.05(0.04) | 13.04(0.05) | 12.74(0.04) | **10.01**(0.03) | 10.45(0.04) | 19.16(0.08) | 60.34(0.50) |
| | 1.00 | 9.64(0.03) | 8.89(0.03) | 10.05(0.04) | 8.01(0.03) | 7.62(0.03) | 8.44(0.04) | 9.38(0.02) | 8.84(0.02) | 8.12(0.03) | 10.29(0.02) | 8.44(0.03) | **7.23**(0.03) | 12.46(0.04) | 38.01(0.26) |

The three charts EWMA-LA, GLRW and NEW are all based on serial data decorrelation, through either a time series model estimation (for methods EWMA-LA and GLRW) or estimation of the covariance function $\gamma(q)$ (for method NEW). Because the decorrelated observation at the current time point is usually a difference between the original observation at that time point and a linear prediction based on all prior original observations (cf., the formula for computing $e_i$ before Expression (4)), a true shift would be more and more difficult to detect based on the decorrelated data if it cannot be detected early. To investigate this aspect of the charts, the positive rates of the three charts obtained from 10,000 replicated simulations in Case III are calculated and presented in Table 5, where the charts are in the same set up as that of Table 2. In this example, only the signals given within the first 50 time points after the shift occurrence are counted, because all charts will eventually give signals in any simulation run. From the table, it can be seen that the true positive rates (i.e., those when $\delta > 0$) of NEW are uniformly higher than those of the other two charts, while its false positive rate (i.e., the one when $\delta = 0$) is lower. So, NEW performs better in this regard.

Table 5: False and true positive rates of the three charts EWMA-LA, GLRW and NEW in Case III under the same set up as that of Table 2. The positive rates are computed from 10,000 replicated simulations and only the signals given within the first 50 time points after the shift occurrence are counted.

| Methods | $\delta = 0$ | 0.25 | 0.5 | 0.75 | 1 |
|---|---|---|---|---|---|
| EWMA-LA | 0.157 | 0.186 | 0.482 | 0.772 | 0.938 |
| GLRW | 0.185 | 0.204 | 0.489 | 0.778 | 0.943 |
| NEW | 0.139 | 0.227 | 0.497 | 0.789 | 0.945 |

**Impact of $m$ and $T_{max}$.** The performance of the proposed CUSUM chart NEW would depend on the IC sample size $m$ and the assumed maximum time range of autocorrelation $T_{max}$. In this part, we study such potential impact. First, in the setup of Table 2, we fix $T_{max}$ at 20 as in previous examples, and let $m$ change among 500, 1,000, 2,000, and 5,000. The calculated optimal $ARL_1$ values of NEW are shown in Figure 1. From the plots in the figure, we can see that: (i) the performance of NEW would improve when $m$ increases, (ii) the performance is stable in Cases IV-VI when $m \geq 1,000$, and (ii) the performance improvement can almost be ignored when $m \geq 2,000$ in all cases considered. This example shows that the proposed chart NEW would perform stably

when the IC sample size is as large as 2,000. This result is consistent with that found in Jones et al. (2001).

Next, we study the impact of $T_{max}$ on the performance of the proposed chart NEW. In the setup of Table 2, we fix $m$ at 2,000, and let $T_{max}$ change among 2, 5, 10, and 20. The calculated optimal $ARL_1$ values of NEW are shown in Figure 2. From the plots, we can see that: (i) the performance of NEW does not change much when $T_{max}$ changes in Case I, (ii) in Cases II, V and VI, the performance of NEW when $T_{max} = 2$ is slightly worse and its performance is almost identical when $T_{max} = 5, 10$ and 20, (iii) in Cases III and IV, the performance of NEW can improve when $T_{max}$ increases, but the improvement is very small when $T_{max} \geq 5$. This example shows that the proposed chart NEW would perform stably when the assumed maximum time range of autocorrelation $T_{max}$ is chosen to be 5 or larger.

# 4 Real Data Application

In this section, we demonstrate our proposed method using a real dataset obtained from the the Climate Prediction Center of the USA (http://www.cpc.ncep.noaa.gov/). This dataset contains observations of the sea surface temperature (SST) in the Nino 3 Region. The Nino 3 Region is within 90W-150W in longitude and 5S-5N in latitude. This region is commonly used by scientists to classify the intensity of El Niño phenomenon. Developing countries that are dependent upon agriculture and fishing, particularly those bordering the Pacific Ocean, are usually most affected by El Niño. So, it is very important to monitor the intensity of El Niño in that region. If something unusual happens (e.g., warming of the ocean surface), the nearby countries should take actions quickly to avoid natural disaster. The dataset can be found in the R package *tseries*. It contains 598 monthly SST observations of the Nino 3 Region in degrees Celsius, collected from January 1950 to October 1999. The data are shown in Figure 3. We use the first 350 observations as the IC dataset, and the remaining observations for Phase II process monitoring. The two parts of the data are separated by a vertical line in the plot. From Figure 3, it can be seen that the IC data look quite stable and the phase II observations seem to have an upward shift around the 390th month. The Augmented Dickey-Fuller (ADF) test and the Phillips-Perron (PP) test for stationarity of the IC dataset both give a $p$-value of 0.01, suggesting that the stationary assumption of the IC dataset is valid in this data.

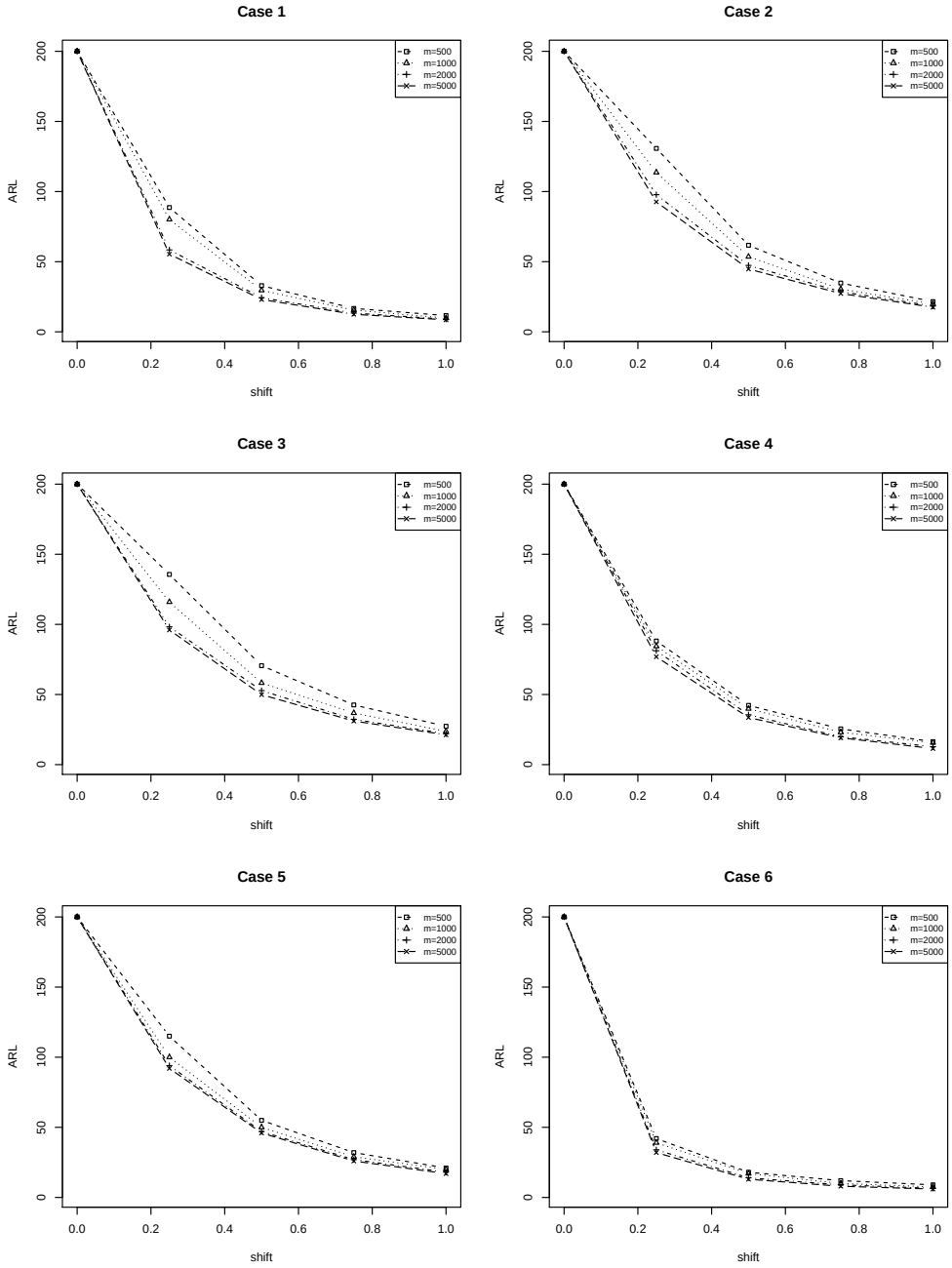


Figure 1: Calculated optimal $ARL_1$ values of the proposed chart NEW when $ARL_0 = 200$, $T_{max} = 20$, the shift size is $\delta\sigma_X$ with $\delta$ changing among 0, 0.25, 0.5, 0.75 and 1.0, and the IC sample size $m$ changes among 500, 1,000, 2,000, and 5,000.

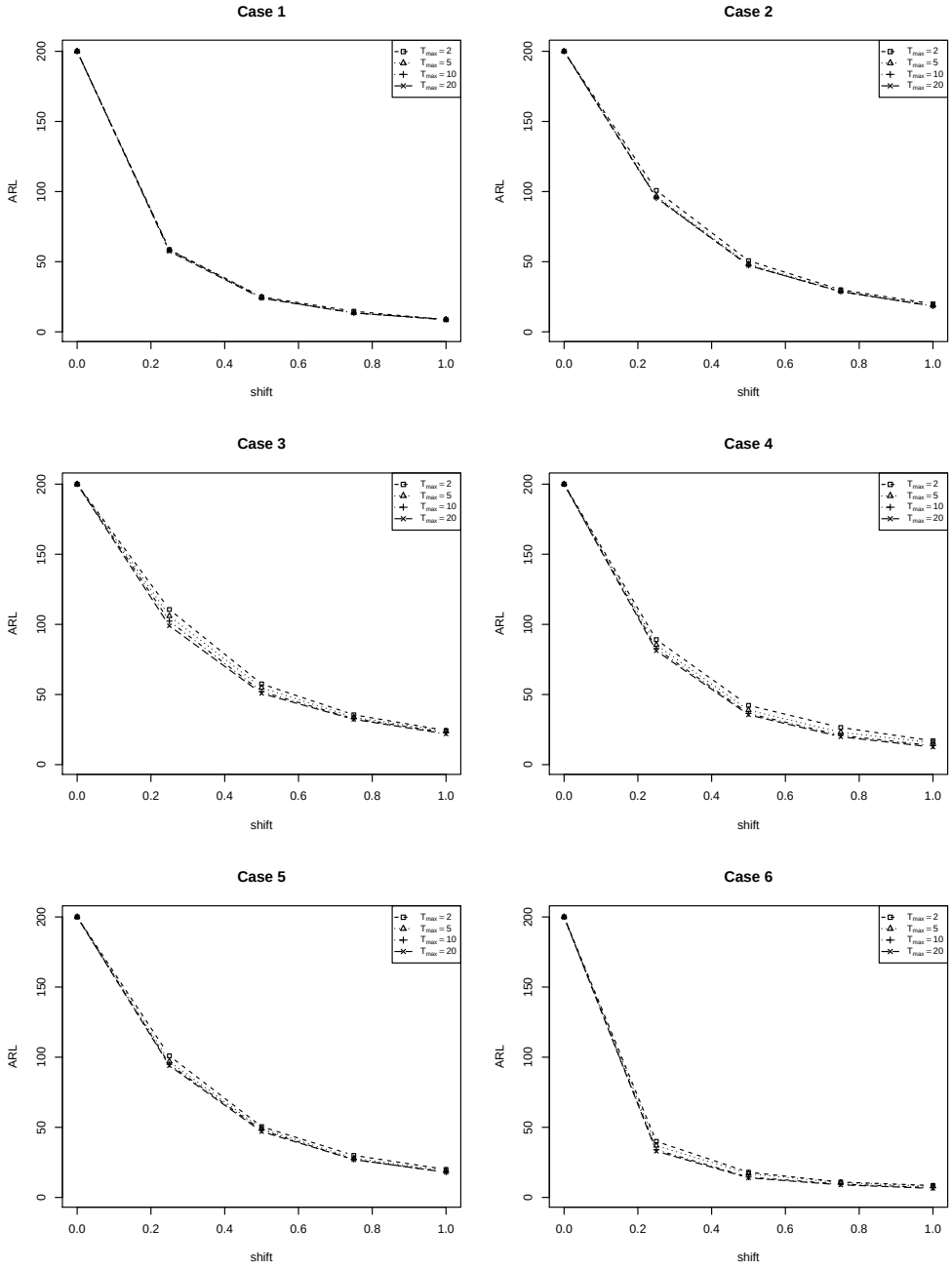


Figure 2: Calculated optimal $ARL_1$ values of the proposed chart NEW when $ARL_0 = 200$, $m = 2,000$, the shift size is $\delta\sigma_X$ with $\delta$ changing among 0, 0.25, 0.5, 0.75 and 1.0, and the assumed maximum time range of autocorrelation $T_{max}$ changes among 2, 5, 10, and 20.

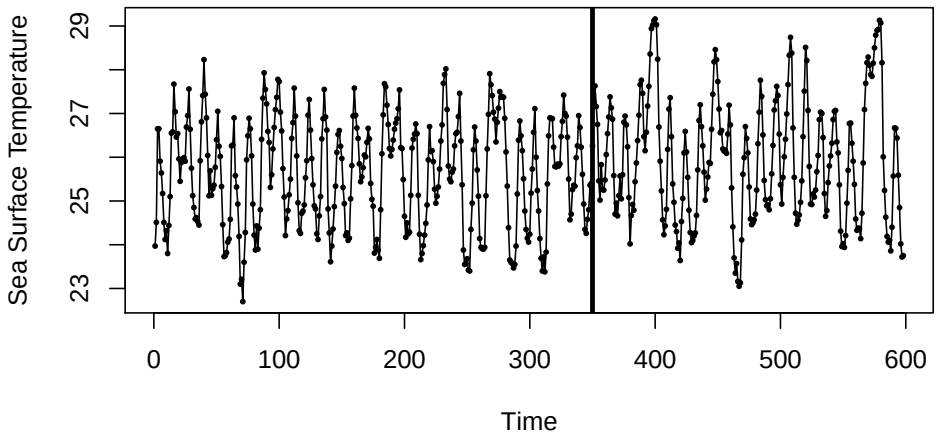


Figure 3: Original observations of the sea surface temperature dataset, where the vertical solid line separates the two parts of the data used as the IC dataset and the Phase II observations, respectively.

Next, we construct the six control charts to monitor the Phase II observations of SST. In all control charts, $ARL_0$ is assumed to be 200. The allowance constants $k$ and $\widetilde{k}$ in CCUSUM and NEW and the weighting parameter $\lambda$ in EWMA-Z and EWMA-LA are all chosen to be 0.2. The window size in GLRW is chosen to be 20 as in the numerical examples in Capizzi and Masarotto (2008). The parameter $p$ in T2 is fixed at 20, as in the simulation examples. To ensure a robust IC performance of the conventional CUSUM chart CCUSUM, its control limit is obtained by the bootstrap procedure in a similar way to that for the proposed chart NEW. The other five charts are set up in the same way as that in the simulation examples. Figure 4 shows the six control charts, where the solid horizontal lines denote the related control limits. From the plots, it can be seen that the proposed chart NEW gives the first signal at the 46th observation (i.e., the 396th observation of the whole dataset). As a comparison, the CCUSUM, EWMA-Z and T2 charts give their first signals at the 48th observation, the EWMA-LA chart gives the first signal the 49th observation, and the chart GLRW gives the first signal at the 47th observation. This example shows that the proposed method NEW is effective in detecting the mean shift in SST, the other five charts are also quite effective in detecting the mean shift, although the signal by GLRW is one month later, the signals by CCUSUM, EWMA-Z and T2 are two months later, and the signal by EWMA-LA is three months later. From the plots in Figure 4, it seems that the evidence of a shift is less convincing in

the charts of EWMA-Z, EWMA-LA and GLRW, because their signals disappear quite fast in the charts.

## 5 Concluding Remarks

Process control for serially correlated data is an important research topic because observed data in SPC applications are often serially correlated. There have been some existing research efforts to tackle this problem. Most existing methods use a parametric time series model to describe the data correlation and a parametric form to describe the data distribution. These methods may not be able to provide a reliable process monitoring when their assumed time series models and the parametric distributions are invalid. In this paper, we try to make another effort to solve this challenging process monitoring problem. A flexible CUSUM chart has been suggested for monitoring serially correlated data. It makes use of the spring length concept by ignoring all history data that are beyond the spring length. It does not require any parametric time series model and/or a parametric process distribution. Numerical studies have shown that it has a reliable IC performance and is effective in detecting process mean shifts in different situations considered. There are still some issues about the proposed method to address in our future research. For instance, in the current proposed chart NEW, we apply the conventional CUSUM chart to the serially decorrelated data. Remember that the conventional CUSUM chart has some optimal properties only when the process observations are independent and normally distributed. The decorrelated observations are linear combinations of the original observations. Their distributions should be closer to normal in many cases, compared to the distributions of the original observations. But, these distributions may still be quite different from normal. In such cases, it is unknown to us whether some more effective control charts can be developed. Also, this paper focuses on univariate processes with continuous numerical observations only. In practice, many processes have multiple quality characteristics involved. Some quality characteristics might take count or categorical values. Thus, online monitoring of serially correlated multivariate processes with numerical or categorical observations requires much future research.

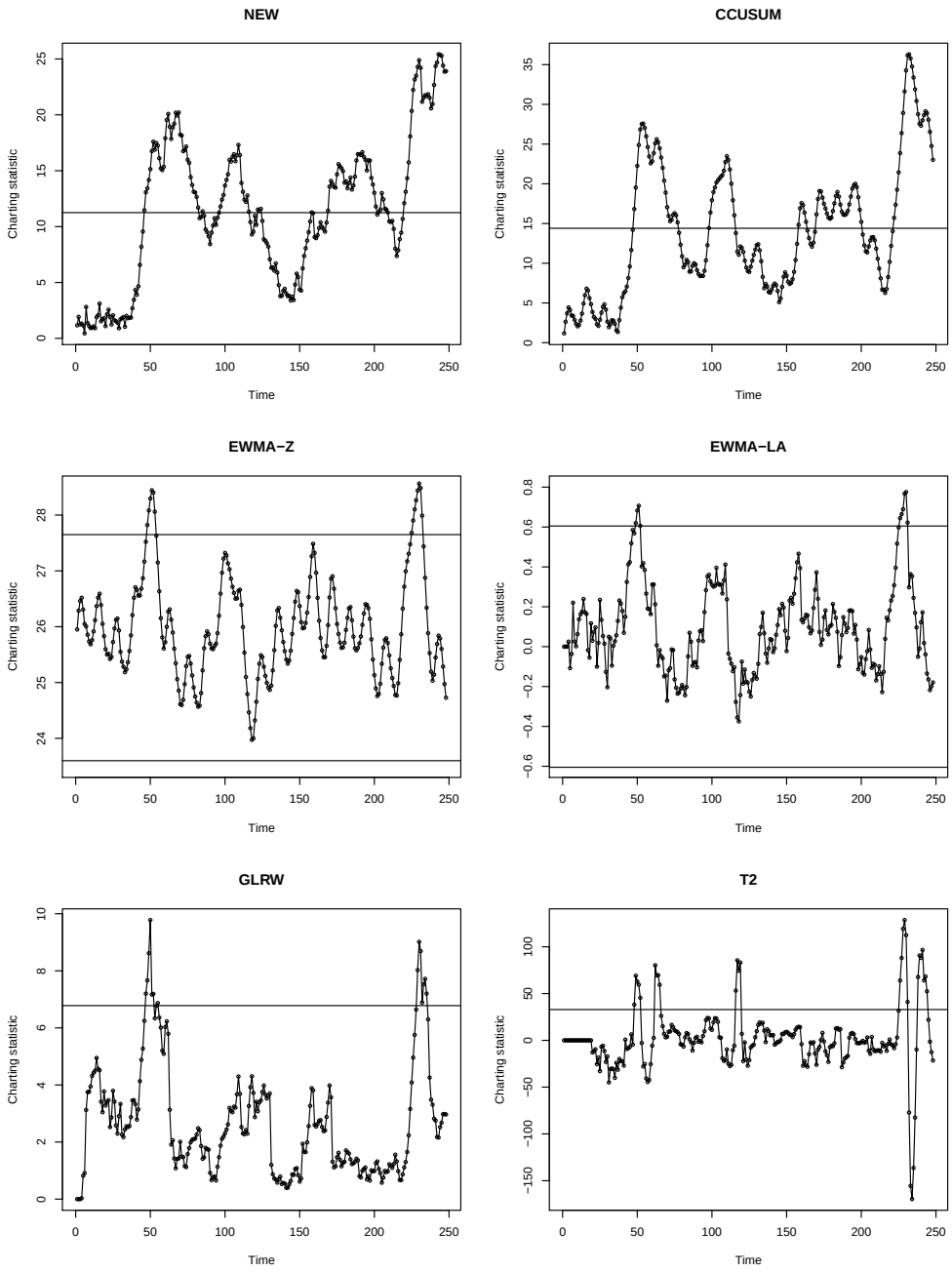


Figure 4: Four control charts applied to the sea surface temperature (SST) data: NEW (upper-left), CCUSUM (upper-right), EWMA-Z (lower-left), and EWMA-LA (lower-right). The horizontal solid lines are the related control limits of the charts.

## Supplementary Materials

**ComputerCodesAndData.zip:** This zip file contains Matlab source code of our proposed method and the real data used in the paper.

**Acknowledgments:** The authors thank the editor, the associate editor, and two referees for many constructive comments and suggestions, which improved the quality of the paper greatly. This research is supported in part by an NSF grant in US, the National Science Fund of China with grant numbers 11771145, 11501209, and 11801210, and the Fundamental Research Funds for the Central Universities and the 111 Project with grant number B14019.

## References

Adams, B.M., and Tseng, I.T. (1998), "Robustness of forecast-based monitoring schemes," *Journal of Quality Technology*, **30**, 328–339.

Alshraideh, H., and Khatatbeh, E. (2014), "A Gaussian process control chart for monitoring autocorrelated process data," *Journal of Quality Technology*, **46**, 317–322.

Apley D.W., and Lee, H.C. (2003), "Design of exponentially weighted moving average control charts for autocorrelated processes with model uncertainty," *Technometrics*, **45**, 187–198.

Apley D.W., and Lee, H.C. (2008), "Robustness comparison of exponentially weighted moving-average charts on autocorrelated data and on residuals," *Journal of Quality Technology*, **40**, 428–447.

Apley D.W., and Shi, J. (1999), "The GLRT for statistical process control of autocorrelated processes," *IIE Transactions*, **31**, 1123–1134.

Apley D.W., and Tsung, F. (2002), "The autoregressive $T^2$ chart for monitoring univariate autocorrelated processes," *Journal of Quality Technology*, **34**, 80–96.

Bakshi, B.R. (1998), "Multiscale PCA with application to multivariate statistical process control," *AIChE Journal*, **44**, 1596–1610.

Berthouex, P.M., Hunter, W.G., and Pallesen, L. (1978), "Monitoring sewage treatment plants: Some quality control aspects," *Journal of Quality Technology,* **10**, 139–149.

Bierens, H.J. (2004), *Introduction to the Mathematical and Statistical Foundations of Econometrics*, Cambridge, UK: Cambridge University Press.

Capizzi, G., and Masarotto, G. (2008), "Practical design of generalized likelihood ratio control charts for autocorrelated data," *Technometrics*, **50**, 357–370.

Capizzi, G., and Masarotto, G. (2016), "Efficient control chart calibration by simulated stochastic approximation," *IIE Transactions*, **48**, 57–65.

Chatterjee, S., and Qiu, P. (2009), "Distribution-free cumulative sum control charts using bootstrap-based control limits," *The Annals of Applied Statistics*, **3**, 349–369.

Efron, B., and Tibshirani, R. (1993), *An Introduction to the Bootstrap,* Boca Raton, FL: Chapman & Hall/CRC.

Harris, T.J., and Ross, W.H. (1991), "Statistical process control procedures for autocorrelated observations," *Canadian Journal of Chemical Engineering*, **69**, 48–57.

Hawkins, D.M., and Olwell, D.H. (1998), *Cumulative Sum Charts and Charting for Quality Improvement*, New York: Springer-Verlag.

He, Z., Wang, Z., Tsung, F., and Shang, Y. (2016), "A control scheme for autocorrelated bivariate binomial data," *Computer & Industrial Engineering*, **98**, 350–359.

Johnson, R.A., and Bagshaw, M. (1974), "The effect of serial correlation on the performance of CUSUM tests," *Technometrics*, **16**, 103–112.

Jones, L.A., Champ, C.W., and Rigdon, S.E. (2001), "The performance of exponentially weighted moving average charts with estimated parameters," *Technometrics*, **43**, 156–167.

Kedem, B., and Fokianos, K. (2002), *Regression Models for Time Series Analysis,* New York: John Wiley & Sons.

Kim, S.H., Alexopoulos, C., Tsui, K.L., and Wilson, J.R. (2007), "A distributionfree tabular CUSUM chart for autocorrelated data," *IIE Transactions*, **39**, 317–330.

Komulainen, T., Sourander, M., and Jm̈sä-Jounela, S.-L. (2004), "An online application of dynamicl PLS to a dearomatization process," *Computers and Chemical Engineering*, **28**, 2611–2619.

Ku, W., Storer, R.H., and Georgakis, C. (1995), "Disturbance detection and isolation by dynamic principal component analysis," *Chemometrics and Intelligent Laboratory Systems*, **30**, 179–196.

Lahiri, S. N. (2013), *Resampling Methods for Dependent Data,* New Yok: Springer-Verlag.

Lee, H. C., and Apley, D. W. (2011), "Improved design of robust exponentially weighted moving average control charts for autocorrelated processes," *Quality and Reliability Engineering International*, **27**, 337–352.

Li, J., and Qiu, P. (2016), "Nonparametric dynamic screening system for monitoring correlated longitudinal data," *IIE Transactions*, **48**, 772–786.

Loredo, E., Jearkpaporn, D., and Borror, C. (2002), "Model-based control chart for autoregressive and correlated data," *Quality and Reliability Engineering International*, **18**, 489–496.

Montgomery, D.C. (2012), *Introduction to Statistical Quality Control*, New York: John Wiley & Sons.

Montgomery, D.C., and Mastrangelo, C.M. (1991), "Some statistical process control methods for autocorrelated data," *Journal of Quality Technology*, **23**, 179–193.

Negiz, A. and Cinar, A. (1997), "Statistical monitoring of multivariable dynamic processes with state-space models," *AIChE Journal*, **43**, 2002–2020.

Qiu, P. (2014), *Introduction to statistical process control,* Boca Raton, FL: Chapman Hall/CRC.

Rato, T.J. and Reis, M.S. (2013), "Advantage of using decorrelated residuals in dynamic principal component analysis for monitoring large-scale systems," *Industrial & Engineering Chemistry Research*, **52**, 13685–13698.

Reis, M.S., Bakshi, B.R., and Saraiva, P.M. (2008), "Multiscale statistical process control using wavelet packets," *AIChE Journal*, **54**, 2366–2378.

Runger, G.C. (2002), "Assignable causes and autocorrelation: control charts for observations or residuals?" *Journal of Quality Technology*, **34**, 165–170.

Runger, G.C., and Willemain, T.R. (1995), "Model-based and model-free control of autocorrelated processes," *Journal of Quality Technology*, **27**, 283–292.

Schimd, W., and Schöne, A. (1997), "Some properties of the EWMA control chart in the presence of autocorrelation," *Annals of Statistics*, **25**, 1277–1283.

Simoglou, A., Martin, E.B.. and Morris, A.J. (1999), "Dynamic multivariable statistical process control using partial least squares and canonical variate analysis," *Computers and Chemical Engineering*, **23**, S277–S280.

Treasure, R.J., Kruger, U., and Cooper, J.E. (2004), "Dynamic multivariate statistical process control using subspace identification," *Journal of Process Control*, **14**, 279–292.

Vander Wiel, S.A. (1996), "Monitoring processes that wander using integrated moving average models," *Technometrics*, **38**, 139–151.

Wardell, D.G., Moskowitz, H., Plante, R.D. (1994), "Run-length distributions of special-cause control charts for correlated processes," *Technometrics*, **36**, 3–17.

Weiß, C.H. (2015), "SPC methods for time-dependent processes of countsA literature review," *Cogent Mathematics*, **2**, 1111116.

Wu, W.B. (2011), "Asymptotic theory for stationary processes," *Statistics and Its Interface*, **4**, 207-226.

Yeh, A.B., Huwang, L., McGrath, R.N., and Zhang, Z. (2010), "On monitoring process variance with individual observations," *Quality and Reliability Engineering International*, **26**, 631–641.

Zhang, N. F. (1998), "A statistical control chart for stationary process data," *Technometrics*, **40**, 24–38.